Reactions of the Homo- and Heterodinuclear Complexes $M_2(CO)_6$(*N*,*N*′-diisopropyl-1,4-diaza-1,3-butadiene) [M_2 = Fe_2, FeRu, Ru_2] with (*N*,*N*-Diethylamino)-1-propyne[1]

Fred Muller, Gerard van Koten, Marco J. A. Kraakman, and Kees Vrieze*

Laboratorium voor Anorganische Chemie, University of Amsterdam, J. H. van't Hoff Instituut, Nieuwe Achtergracht 166, 1018 WV Amsterdam, The Netherlands

Dick Heijdenrijk and Martin C. Zoutberg

Laboratorium voor Kristallografie, University of Amsterdam, J. H. van't Hoff Instituut, Nieuwe Achtergracht 166, 1018 WV Amsterdam, The Netherlands

Received August 24, 1988

The reactions of $M_2(CO)_6$(*i*-Pr-DAB) [**1a**, M_2 = Fe_2; **1b**, M_2 = FeRu; **1c**, M_2 = Ru_2; R-DAB = RN=CHCH=NR], in which the DAB ligand is in the σ-N,μ_2-N′,η^2-C=N′ 6e donating bridging coordination mode, with (*N*,*N*-diethylamino)-1-propyne (DEAP), have been investigated. Reaction of the diiron complex **1a** with DEAP at 69 °C afforded the ferracyclopentadienyl complex Fe_2[MeC=C(NEt_2)C(Me)=$CNEt_2$]$(CO)_4$(*i*-Pr-DAB) (**6a**) containing two head-to-tail coupled alkyne molecules. The same reaction at 20 °C produces the complex $Fe_2(CO)_5$[*i*-PrNCHCHN(*i*-Pr)C(O)C(Me)=$CNEt_2$] (**8a**), of which the crystal structure has been determined. Red crystals of **8a** ($Fe_2C_{21}H_{29}N_3O_6$, M_r = 531.17, Z = 4) are triclinic, space group $P\bar{1}$, and have cell constants a = 14.115 (2) Å, b = 14.279 (3) Å, c = 13.168 (2) Å, α = 95.337 (14)°, β = 107.444 (17)°, and γ = 102.916 (22)°. A total of 2788 reflections (Mo Kα, μ = 12.31 cm^{-1}) were used in the refinement which converged to a final R value of 0.064. The structure consists of an $Fe_2(CO)_5$ core [Fe–Fe = 2.576 (3) Å, all CO's terminally bonded] bridged by an organic ligand resulting from the C–C coupling of the CMe moiety of the alkyne to a CO, to which one of the R-DAB N atoms is N-C coupled. The ligand is further bonded to the Fe carbonyl core via a C–Fe σ-bond, the σ-bonded N–C coupled N atom, and an azaallyl fragment. The reaction of the heterodinuclear complex **1b** with DEAP afforded only one product, FeRu$(CO)_5$(*i*-Pr-DAB)(MeC≡$CNEt_2$) (**3b**), that according to the crystal structure determination consists of a chelating DAB ligand bonded to the Ru center of the FeRu$(CO)_5$ fragment. The latter fragment is bridged by the alkyne molecule which is bonded via a μ_2-carbene CMe and a terminal $CNEt_2$ carbene fragment. Yellow crystals of **3b** ($FeRuC_{20}H_{29}N_3O_5$, M_r = 548.38, Z = 8) are monoclinic, space group $P2_1/n$, and have cell constants a = 17.405 (2) Å, b = 17.716 (4) Å, c = 17.013 (2) Å, β = 108.06 (1)°. A total of 4901 reflections (Mo Kα, μ = 12.06 cm^{-1}) were used in the refinement which converged to a final R value of 0.053. The reaction of the diruthenium complex **1c** with DEAP at 20 °C afforded $Ru_2(CO)_5$(*i*-Pr-DAB)(MeC≡$CNEt_2$) (**3c**) which based on IR and NMR data is proposed to be isostructural to **3b**. This reaction is the first example of a reaction of $Ru_2(CO)_6$(α-diimine) with an alkyne, in which the η^2-C=N bonded imine fragment is substituted by the alkyne and no C—C bond formation between the alkyne and the DAB ligand occurs. This indicates that the electronic properties of the alkyne in reactions of $M_2(CO)_6$(L) [L = R-DAB, R-Pyca] with alkynes have a major influence on the course of the reaction.

Introduction

Recently we have been involved in a detailed and systematic study of reactions of alkynes with the homo- and heterodinuclear carbonyl α-diimine complexes $M_2(CO)_6$(L) [M_2 = Fe_2, FeRu, Ru_2; L = R-DAB (RN=CHCH=NR), R-Pyca (C_5H_4N-2-CH=NR)], in which the α-diimine ligand is bridging the $M_2(CO)_6$ core in the 6e donating σ-N,μ_2-N′,η^2-C=N′ bonding mode.[3] The observed reactivity appeared to be strongly influenced not only by the nature of the metal and the η^2-C=N-M interaction[2] but also by the properties of the alkyne substituents. Via a systematic investigation of the reactivities of ethyne and mono- and disubstituted alkynes in reactions with the above-mentioned metal α-diimine complexes the influence of the alkyne properties on the course of the reactions could be studied.[3] This investigation, however, was limited to alkynes with either weakly or strongly electron-withdrawing substituents like phenyl, methoxycarbonyl, or trifluoromethyl groups. In order to obtain a better view of the influence of the electronic properties of the alkyne on the product distribution, we have studied the reactivity of the comparable and isostructural complexes $M_2(CO)_6$(*i*-Pr-DAB) [M_2 = Fe_2 (**1a**), FeRu (**1b**), Ru_2 (**1c**)] toward (*N*,*N*-diethylamino)-1-propyne (DEAP). Contrary to the alkynes with electron-withdrawing substituents, in DEAP the alkyne C atoms have a δ^- polarization. The observed reactions can be compared to those of $M_3(CO)_{12}$ [M = Fe, Ru] with the same alkyne, reported recently by Daran et al.[4]

* To whom correspondence should be addressed.

(1) Reactions of Dinuclear Metal Carbonyl α-Diimine Complexes with Alkynes. 8. Part 7: see ref 2.

(2) Muller, F.; van Koten, G.; Kraakman, M. J. A.; Vrieze, K.; Zoet, R.; Duineveld, C. A. A.; Heijdenrijk, D.; Stam, C. H.; Zoutberg, M. C. *Organometallics*, in press.

(3) (a) Muller, F.; Vrieze, K. *Coordination Chemistry and Catalysis*: Ziolkowski, J. J., ed.; World Scientific Publishing Co.: Singapore, 1988. (b) Elsevier, C. J.; Muller, F.; Vrieze, K.; Zoet, R. *New J. Chem.* **1988**, *12*, 571. (c) Part 1 of this series: Muller, F.; van Koten, G.; Vrieze, K.; Heijdenrijk, D. *Inorg. Chim. Acta* **1989**, *158*, 81. (d) Part 2 of this series: Muller, F.; van Koten, G.; Vrieze, K.; Heijdenrijk, D. *Organometallics* **1989**, *8*, 33. (e) Part 3 of this series: Muller, F.; van Koten, G.; Vrieze, K.; Heijdenrijk, D.; Krijnen, L. B.; Stam, C. H. *Organometallics* **1989**, *8*, 41. (f) Part 4 of this series: Muller, F.; Han, I. M.; van Koten, G.; Vrieze, K.; Heijdenrijk, D.; de Jong, R. L.; Zoutberg, M. C. *Inorg. Chim. Acta* **1989**, *158*, 69. (g) Part 5 of this series: Muller, F.; Han, I. M.; van Koten, G.; Vrieze, K.; Heijdenrijk, D.; van Mechelen, J.; Stam, C. H. *Inorg. Chim. Acta* **1989**, *158*, 99. (h) Part 6 of this series: Muller, F.; van Koten, G.; Vrieze, K.; Duineveld, C. A. A.; Heijdenrijk, D.; Mak, A. N. S.; Stam, C. H. *Organometallics*, preceding paper in this issue. (i) Muller, F.; van Koten, G.; Vrieze, K.; Heijdenrijk, D.; Krijnen, L. B.; Stam, C. H. *J. Chem. Soc., Chem. Commun.* **1986**, 150.

(4) (a) Cabrera, E.; Daran, J.-C.; Jeannin, Y.; Kristiansson, O. *J. Organomet. Chem.* **1986**, *310*, 367. (b) Daran, J.-C.; Jeannin, Y. *Organometallics* **1984**, *3*, 1158.

0276-7333/89/2308-1331$01.50/0

Table I. IR and FI Mass Data and Elemental Analyses of $FeRu(CO)_5(i\text{-Pr-DAB})(MeC_2NEt_2)$ (3b), $Ru_2(CO)_5(i\text{-Pr-DAB})(MeC_2NEt_2)$ (3c), $Fe_2(CO)_5[i\text{-PrNCHCHN}(i\text{-Pr})C(O)C(Me)=CNEt_2]$ (8a), and $Fe_2[MeC=C(NEt_2)C(Me)=CNEt_2](CO)_4(i\text{-Pr-DAB})$ (6a)

			elemental analysis					
			C		H		N	
compd	IR ν_s(C=O),[a] cm^{-1}	FI mass (calcd)[b]	obsd	calcd	obsd	calcd	obsd	calcd
3b	2003 (m), 1971 (vs), 1932 (s), 1918 (m), 1603 (w)	549 (548.38)	43.49	43.81	5.20	5.33	7.66	7.66
3c	2021 (m), 1974 (vs), 1945 (s), 1919 (m), 1593 (w)	594 (593.61)	40.53	40.47	5.04	4.92	7.12	7.08
6a	2030 (s), 1958 (vs), 1847 (s)	587 (586.34)	51.96	53.26	7.26	7.22	9.56	9.09
8a	2036 (s), 1990 (s), 1968 (s), 1948 (m), 1652 (m)	503[c] (531.17)	46.59	47.48	5.42	5.50	7.76	7.91

[a] Measured in hexane solution. Abbreviations: vs, very strong; s, strong; m, medium; w, weak; vw, very weak. [b] Based on ^{56}Fe and ^{101}Ru. [c] $M^+ - CO$.

Table II. ^1H NMR Data of $FeRu(CO)_5(i\text{-Pr-DAB})(MeC_2NEt_2)$ (3b), $Ru_2(CO)_5(i\text{-Pr-DAB})(MeC_2NEt_2)$ (3c), $Fe_2(CO)_5[i\text{-PrNCHCHN}(i\text{-Pr})C(O)C(Me)=CNEt_2]$ (8a), and $Fe_2[MeC=C(NEt_2)C(Me)=CNEt_2](CO)_4(i\text{-Pr-DAB})$ (6a)[a]

compd	*i*-Pr Me	*i*-Pr CH	N–CH	Et	Me
3b[b]	1.17, 1.21 (d, d, 6 Hz)	4.43 (sept, 6 Hz)	7.51 (s)	1.02, 1.20 (t, t, 5 Hz), 3.2–3.8 (4 × q, 5 Hz)	2.33 (s)
3b[c]	0.8–1.3 (m)[d]	4.17 (sept, 6 Hz), 4.68 (sept, 6 Hz)	7.19 (s), 7.38 (s)	0.8–1.3 (m), 2.9–3.9 (4 × q, 5 Hz)	2.32 (s)
3c[e]	1.37, 1.43 (d, d, 6 Hz)	4.63 (sept, 6 Hz)	7.97 (s)	1.27 (t, 7 Hz), 3.70 (q, 7 Hz)	2.39 (s)
3c[f]	1.37, 1.43 (d, d, 6 Hz)	4.30 (sept, 6 Hz), 4.74 sept, 6 Hz)	7.87 (s), 7.96 (s)	1.27 (t, 7 Hz), 3.70 (q, 7 Hz)	2.39 (s)
6a[g]	0.9–1.4 (m)	3.88 (sept, 6 Hz), 4.78 (sept, 6 Hz)	7.86 (s), 8.20 (s)	0.9–1.4 (m), 3.13 (m)	1.99 (s), 2.26 (s)
8a[h]	0.90, 0.93, 1.18 (d, d, d, 6 Hz)	3.65 (sept, 6 Hz), 3.76 (sept, 6 Hz)	5.64[i], 3.87[i]	0.86, 1.14 (t, 7 Hz), 2.82, 2.97, 3.26, 3.41 (4 × q, 7 Hz)	1.73 (s)

[a] Values in ppm relative to Me_4Si, spectrometer frequency: 100 MHz. [b] Measured in toluene-d_8 solution, 350 K. [c] Measured in toluene-d_8 solution, 243 K. [d] Not resolved. [e] Measured in CD_2Cl_2 solution, 293 K. [f] Measured in CD_2Cl_2 solution, 173 K. [g] Measured in $CDCl_3$ solution, 263 K. [h] Measured in toluene-d_8 solution, 293 K. [i] Azaallyl protons, dd, 2 Hz.

Experimental Section

Materials and Apparatus. ^1H and ^{13}C NMR spectra were recorded on Bruker AC100 and WM250 spectrometers. IR spectra were measured with a Perkin-Elmer 283 spectrometer. The field ionization (FI) mass spectra were obtained with a Varian MAT711 double-focusing mass spectrometer with a combined EI/FI/FD source. The samples were dissolved in dichloromethane and introduced via the direct insertion probe into the ion source, of which the temperature was generally 80–100 °C. Elemental analyses were carried out by the section Elemental Analysis of the Institute for Applied Chemistry, TNO, Zeist, The Netherlands.

All preparations were carried out in an atmosphere of purified nitrogen, using carefully dried solvents. All column chromatography was performed by using silica gel (60 Mesh, dried and activated before use) as the stationary phase. $Fe_2(CO)_6$(*i*-Pr-DAB) (**1a**),[5] $FeRu(CO)_6$(*i*-Pr-DAB) (**1b**),[6] and $Ru_2(CO)_6$(*i*-Pr-DAB) (**1c**)[5a] and (*N*,*N*-diethylamino)-1-propyne (DEAP)[7] were prepared according to known procedures. The products were identified by IR- and mass spectrometry, by elemental analyses (Table I) and by ^1H (Table II) and ^{13}C NMR (Table III).

Synthesis of $FeRu(CO)_5(i\text{-Pr-DAB})(MeC{\equiv}CNEt_2)$ (3b). A solution of $FeRu(CO)_6$(*i*-Pr-DAB) (**1b**) (2 mmol, 930 mg) and DEAP (6 mmol, 666 mg) in 100 mL of hexane was refluxed for 90 min, during which the brown-red color of the solution changed to purple. The obtained reaction mixture was evaporated to dryness, and the crude reaction product was purified by column chromatography. Elution with hexane/diethyl ether (9:1) produced a purple fraction, which was concentrated to 50 mL. Crystallization at −80 °C afforded **3b** as dark purple crystals, suitable for X-ray crystallography, in 85% yield. The crystals were collected by decanting the mother liquor and were dried in vacuo.

Synthesis of $Ru_2(CO)_5(i\text{-Pr-DAB})(MeC{\equiv}CNEt_2)$ (3c). A solution of $Ru_2(CO)_6$(*i*-Pr-DAB) (**1c**) (1.5 mmol, 765 mg, prepared in situ) and DEAP (1.7 mmol, 189 mg) in 50 mL of heptane was stirred at 20 °C for 20 h, during which the yellow-orange color of the solution changed to purple. The obtained reaction mixture was evaporated to dryness, and the crude product was purified by column chromatography. Elution with hexane/diethyl ether (9:1) afforded an intensely colored purple fraction which was concentrated to 40 mL. Crystallization at −80 °C produced purple crystals of **3c** in 60% yield. The crystals were collected by decanting the mother liquor and were dried in vacuo.

Table III. ^{13}C NMR Data of $FeRu(CO)_5(i\text{-Pr-DAB})(MeC_2NEt_2)$ (3b), $Ru_2(CO)_5(i\text{-Pr-DAB})(MeC_2NEt_2)$ (3c), $Fe_2(CO)_5[i\text{-PrNCHCHN}(i\text{-Pr})C(O)C(Me)=CNEt_2]$ (8a), and $Fe_2[MeC=C(NEt_2)C(Me)=CNEt_2](CO)_4(i\text{-Pr-DAB})$ (6a)[a]

3b 13.5, 13.7 (NEt_2 Me); 23.4, 24.6, 26.0, 26.3 (*i*-Pr Me); 26.0 (C≡C*Me*); 49.7, 50.4 (NEt_2 CH_2); 58.6, 65.5 (*i*-Pr CH); 88.7 (C≡*C*Me); 146.7, 147.9 (N=CH); 200.0, 208.9 (CO Ru) 218.0 (3 × CO Fe); 232.9 (*C*=CMe) [$CDCl_3$, 243 K, 25 MHz]

3b 13.3, 13.4 (NEt_2 Me); 24.7, 26.5 (*i*-Pr Me); 25.1 (C≡C*Me*); 49.9, 50.5 (NEt_2 CH_2); 62.0 (*i*-Pr CH); 147.2 (N=CH); 201.1, 208.2 (CO Ru) 217.7 (3 × CO Fe); 234.6 (*C*=CMe) [toluene-d_8, 323 K, 25 MHz]

3c 13.4, 13.5 (NEt_2 Me); 23.9, 25.0, 26.9, 28.4 (*i*-Pr Me); 25.7 (C≡C*Me*); 49.4, 51.1 (NEt_2 CH_2); 59.0, 65.7 (*i*-Pr CH); 80.4 (C≡*C*Me); 144.5, 146.3 (N=CH); 201.8, 211.6 (CO Ru) 218.0 (3 × CO Fe); 223.2 (*C*≡CMe) [CD_2Cl_2, 193 K, 25 MHz]

6a 15.1 (2×, NEt_2Me); 19.0, 22.0, 22.7, 26.1 (*i*-Pr Me); 27.9, 30.9 (C≡C*Me*); 47.1, 47.4 (NEt_2 CH_2); 58.4, 59.8 (*i*-Pr CH); 116.3, 152.7 (C≡*CC*=C); 165.1, 199.6 (*C*=CC=*C*); 211.9, 216.5, 217.1 (CO) [$CDCl_3$, 263 K, 25 MHz]

8a 13.8, 14.4 nNEt_2 Me); 16.0, 18.8, 21.0, 22.3 (*i*-Pr Me); 31.4 (C≡C*Me*); 51.2 (2 × NEt_2 CH_2); 58.5, 61.9 (*i*-Pr CH); 69.2 (*C*HCHN); 95.3 (CH*C*HN); 102.3 (C≡*C*Me); 180.7 (*C*≡CMe); 212.9 (NC=O); 213.8 (3 × CO); 216.3, 221.6 (CO) [$CDCl_3$, 263 K, 63 MHz]

[a] Values in ppm, relative to Me_4Si.

Synthesis of $Fe_2(CO)_5[i\text{-PrNCHCHN}(i\text{-Pr})C(O)C(Me)=CNEt_2]$ (8a). A solution of $Fe_2(CO)_6$(*i*-Pr-DAB) (**1a**) (2 mmol, 840 mg) and DEAP (6 mmol, 666 mg) in 50 mL of hexane was stirred for 30 h. The crude reaction mixture was evaporated to dryness and separated by column chromatography. Elution with

(5) (a) Staal, L. H.; Polm, L. H.; Balk, R. W.; van Koten, G.; Vrieze, K.; Brouwers, A. M. F. W. *Inorg. Chem.* **1980**, *19*, 3343. (b) Frühauf, H.-W.; Landers, A.; Goddard, R.; Krüger, K. *Angew. Chem., Int. Eng. Ed.* **1978**, *17*, 64.

(6) Zoet, R.; van Koten, G.; Muller, F.; Vrieze, K.; van Wijnkoop, M.; Goubitz, K; van Halen, C. J. G.; Stam, C. H. *Inorg. Chim. Acta* **1988**, *149*(2), 193.

(7) Brandsma, L. *Preparative Acetylenic Chemistry*; Elsevier: Amsterdam, 1971; p 146.

Scheme I. Reactions of $M_2(CO)_6(i\text{-Pr-DAB})$[$M_2$ = Fe_2, FeRu, Ru_2] with $MeC{\equiv}CNEt_2$[a]

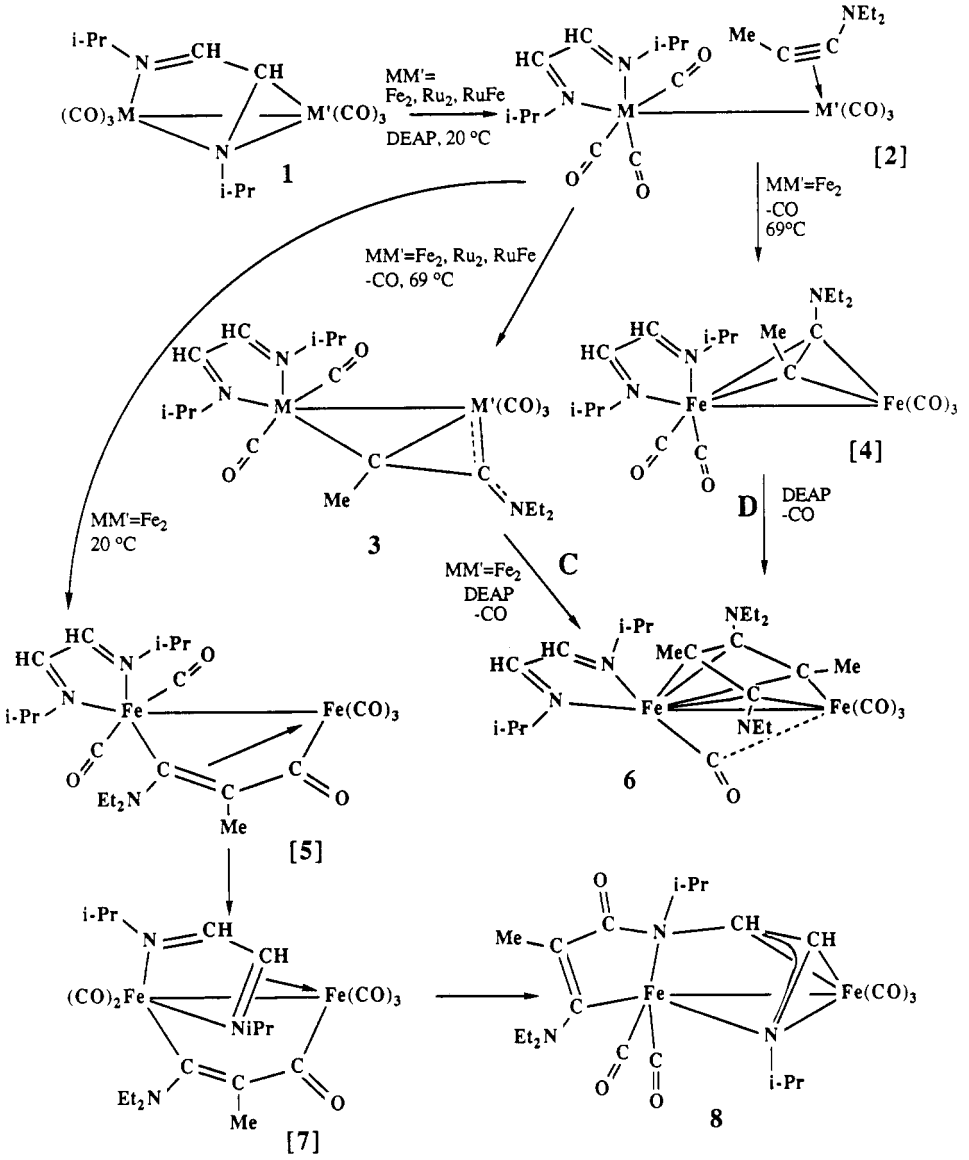

[a] Structures **2**, **4**, **5**, and **7** are proposed intermediates.

diethyl ether afforded the orange-red **8a** in 80% yield. Crystallization from hexane at −80 °C produced dark red crystals suitable for X-ray crystallography. The crystals were collected by decanting the mother liquor, washed with 20 mL of hexane, and dried in vacuo.

Synthesis of Fe_2[MeC=C(NEt_2)C(Me)=CNEt_2]$(CO)_4$(*i*-Pr-DAB) (6a). A solution of **1a** (2 mmol, 840 mg) and DEAP (6 mmol, 666 mg) in 50 mL of hexane was refluxed for 3 h. The solvent was removed in vacuo, and the crude product was purified by column chromatography. Elution with hexane/diethyl ether (9:1) afforded the purple complex **6a** in about 60% yield. Further purification proceeded by recrystallization from hexane at −80 °C.

Crystal Structure Determinations of $FeRu(CO)_5$(*i*-Pr-DAB)(MeC≡CNEt_2) (3b) and $Fe_2(CO)_5$[*i*-PrNCHCHN(*i*-Pr)C(O)C(Me)=CNEt_2] (8a). The crystallographic data of complexes **3b** and **8a** are listed in Table IV. The reflections were measured on a Nonius CAD4 diffractometer (25 °C, θ–2θ scan). Those with an intensity below the $2.5\sigma(I)$ level were treated as unobserved. The structures were solved by means of the heavy-atom method. The Fe atoms of both complexes were located by using the symbolic addition program set SIMPEL.[8] The C, N, and O atomic positions were derived from ΔF-Fourier syntheses. The positions of the H atoms of **3b** were calculated and not refined; the H atoms of **8a** were excluded. The refinement of the non-hydrogen atoms proceeded by using anisotropic block-diagonal least-squares calculations. An empirical absorption correction (DIFABS)[9] was applied. The calculations were performed with XRAY76;[10] the atomic scattering factors were taken from Cromer and Mann (1968)[11] and the dispersion correction factors from ref 12.

Results and Discussion

The reaction of $Fe_2(CO)_6(i\text{-Pr-DAB})$ (**1a**) with (*N*,*N*-diethylamino)-1-propyne (DEAP) at 20 °C in hexane solution affords in high yield as the single product the complex $Fe_2(CO)_5$[*i*-PrNCHCHN(*i*-Pr)C(O)C(Me)=CNEt_2] (**8a**). In this complex, of which the X-ray single-crystal

(8) Overbeek, A. R.; Schenk, H. *Computing in Crystallography*; Schenk, H., Olthof-Hazekamp, R., van Koningsveld, H., Bassi, G. C., Eds.; University Press: Delft, 1978.

(9) Walker, N.; Stuart, D. *Acta Crystallogr., Sect. A* **1983**, *A39*, 158.

(10) Stewart, J. M. The XRAY76 system; Technical Report TR446; Computer Science Center, University of Maryland: College Park, MD, 1976.

(11) Cromer, D. T.; Mann, J. B. *Acta Crystallog., Sect. A* **1968**, *A24*, 321.

(12) *International Tables for X-Ray Crystallography*; Kynoch Press: Birmingham, 1974; Vol. IV.

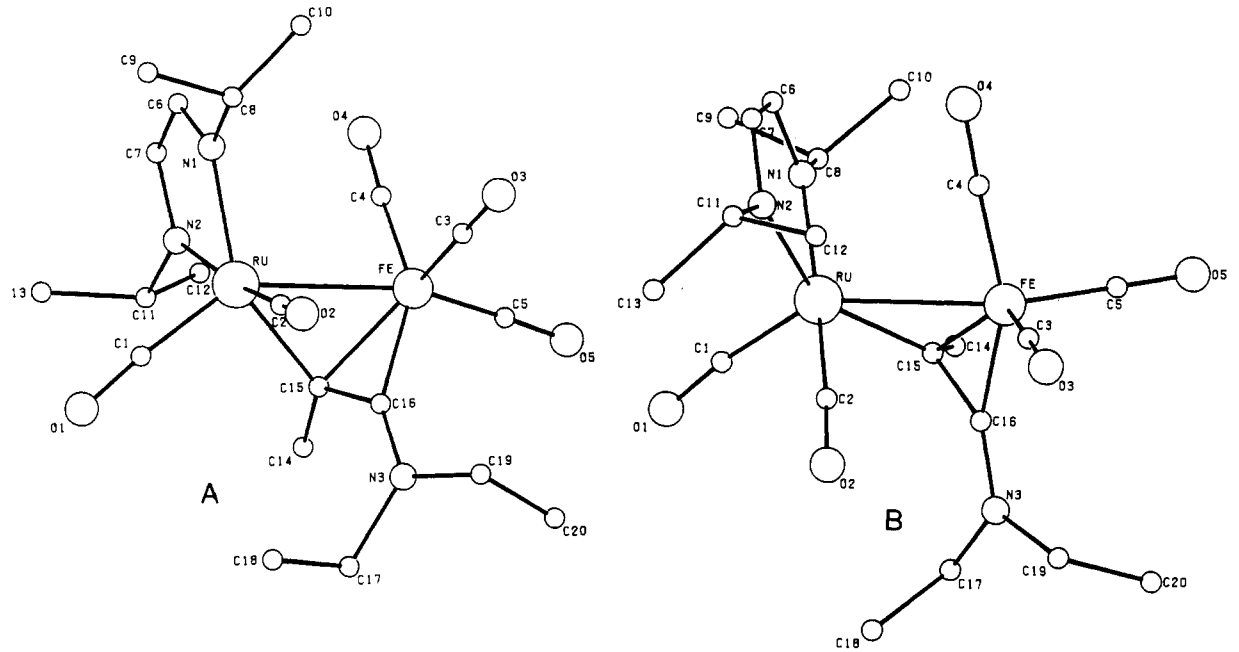

Figure 1. PLUTO drawing of both molecules of $FeRu(CO)_5(i\text{-Pr-DAB})(MeC_2NEt_2)$ (**3b**). The H atoms are omitted for clarity.

Table IV. Crystallographic Data of $FeRu(CO)_5(i\text{-Pr-DAB})(MeC_2NEt_2)$ (3b) and $Fe_2(CO)_5[i\text{-PrNCHCHN}(i\text{-Pr})C(O)C(Me)=CNEt_2]$ (8a)

	3b	8a
formula, mol wt	$FeRuC_{20}H_{29}N_3O_5$, M_r = 548.38	$Fe_2C_{21}H_{29}N_3O_6$, M_r = 531.17
cryst system	monoclinic	triclinic
space group	$P2_1/n$	$P\bar{1}$
a, Å	17.405 (2)	14.115 (2)
b, Å	17.716 (4)	14.279 (3)
c, Å	17.013 (2)	13.168 (14)
α, deg	90	95.337 (14)
β, deg	108.06 (1)	107.444 (17)
γ, deg	90	102.916 (21)
V, Å^3	4988	2431
d_{calcd}, g·cm^3; Z	1.46; 8	1.45; 4
μ, cm^{-1}	12.06	12.31
cryst color, size, mm^3	purple, 0.35 × 0.20 × 0.50	red, 0.28 × 0.13 × 0.38
radiatn	Mo Kα, λ = 0.71069 Å	Mo Kα, λ = 0.71069 Å
2θ range, deg	2.2–50	2.2–44
no. of reflctns	9024	5906
no. of reflctns with $I < 2.5\sigma(I)$	4123	3117
no. of reflctns in refinement	4901	2788
h min, max	−20, 20	−14, 14
k min, max	0, 20	−15, 15
l min, max	0, 20	0, 13
abs cor	DIFABS[9]	DIFABS[9]
extinctn corr	isotropic	isotropic
weighting scheme	unit weights	unit weights
anomalous scattering	Fe, Ru	Fe
final R, R_w	0.053, ...	0.064, ...

structure has been determined, the CMe moiety of the alkyne is coupled to a CO molecule, which is C–N coupled to the σ-bonded N atom of the R-DAB ligand. The remaining three atoms of the latter ligand form an azaallylic fragment which is bonded to the second Fe center (see Scheme I).

Reaction of **1a** at 69 °C with DEAP in hexane solution affords as the main product $Fe_2[MeC{=}C(NEt_2)C(Me){=}CNEt_2](CO)_4(i\text{-Pr-DAB})$ (**6a**) (see Scheme I). On the basis of IR ^1H and ^{13}C NMR data, we concluded that this complex is isostructural to $Fe_2[HC{=}C(C(O)OMe)C(H){=}C(O)OMe](CO)_4(i\text{-Pr-DAB})$,[3f] formed in the thermal reaction of **1a** with methyl propynoate. The crystal structure of this latter complex showed that two head-to-tail coupled alkynes form with one of the Fe centers a ferracyclopentadienyl fragment, which is bonded to a $Fe(CO)(\sigma,\sigma\text{-}N,N'\text{-}i\text{-Pr-DAB})$ fragment.[3f]

$FeRu(CO)_6(i\text{-Pr-DAB})$ (**1b**) does not react with DEAP at 20 °C. When, however, this reaction is performed in refluxing hexane, the complex $FeRu(CO)_5(i\text{-Pr-DAB})(MeC{\equiv}CNEt_2)$ (**3b**) is formed in high yield. In this complex, as was revealed by the X-ray crystal structure, the DAB ligand is chelate bonded to the $Ru(CO)_2$ center. The alkyne is in a bridging position between Fe and Ru and bonded in the same fashion as was earlier observed in $Fe_2(CO)_7(MeC{\equiv}CNEt_2)$.[4a] No products resulting from the coupling of the alkyne either to the DAB ligand or to a second alkyne molecule were observed.

From the reaction of $Ru_2(CO)_6(i\text{-Pr-DAB})$ (**1c**) with DEAP at 20 °C $Ru_2(CO)_5(i\text{-Pr-DAB})(MeC{\equiv}CNEt_2)$ (**3c**) was isolated (see Scheme I). This product is analogous to that of the reaction of **1b** with DEAP, although this latter reaction only proceeded at higher temperatures. Also in the reaction of **1c** with DEAP no other products were formed. When this reaction was performed at higher temperatures, extensive decomposition occurred and no defined products could be isolated.

Molecular Structure of $FeRu(CO)_5(i\text{-Pr-DAB})(MeC{\equiv}CNEt_2)$ (3b). The unit cell of **3b** contains two sets of two independent molecules. The structures of the independent molecules differ with respect to the orientation of the alkyne ethyl groups and the DAB isopropyl groups (see Figure 1). Molecule A shows the normally observed geometry of a chelating i-Pr-DAB ligand with both i-Pr methine C—H bonds anti with respect to the imine C=N bond. In molecule B, however, one of the i-Pr groups is present in the other rotamer conformation which has the methine C-H bond syn with respect to the corresponding C=N bond. We assume that this is due to crystal packing effects and is not the result of a different bonding of the DAB ligand or the alkyne to the metal carbonyl core in molecule B when compared to molecule A. We will therefore only use one of these molecules (A) in the discussion of the molecular structure of **3b**.

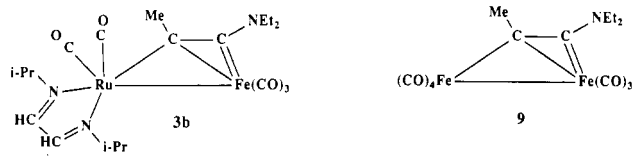

Figure 2. Compounds **3b** and **9**.

The molecular structure of **3b** consists of an $Fe(CO)_3$ unit and a $Ru(CO)_2$(*i*-Pr-DAB) fragment which are linked by a single Fe–Ru bond [Fe–Ru = 2.693 (1) Å][13] and are bridged by a DEAP molecule.

As mentioned above, the alkyne in **3b** is bonded to the metal carbonyl core in the same fashion as in $Fe_2(CO)_7$-(MeC≡CNEt$_2$) (**9**), reported by Daran et al. (see Figure 2.)[4a] In this latter isoelectronic compound there is an $Fe(CO)_4$ unit where in **3b** there is a $Ru(CO)_2$(*i*-Pr-DAB) fragment.

Daran et al. described the bonding of the alkyne in **9** as follows: the CMe moiety of the alkyne acts as a bridging carbene (or methylene) fragment, while the CNEt$_2$ moiety is bonded to one Fe center as a terminal carbene ligand. The bond lengths in **3b** between the alkyne and the metal carbonyl core [C(15)–Ru = 2.134 (7) Å (2.030 (8) Å); C-(15)–Fe = 2.037 (7) Å (2.007 (9) Å); Fe–C(16) = 1.869 (7) Å (1.878 (8) Å) (values for the comparable bonds in **9** in parentheses)] as well as the bond angles around C(15) and C(16) (see Table VII) seem to be in agreement with this description.

The short C–N distance in **9** between the alkyne C(16) atom and the NEt$_2$ group of 1.31 (1) Å indicates a bond order exceeding one. This is in agreement with the presence of an absorption at 1460 cm^{-1} in its IR spectrum. Also in the IR spectrum of **3b** there is a band at 1603 cm^{-1} due to the partially double N(3)–C(16) bond. The higher frequency with respect to **9** can be related to the somewhat shorter N(3)–C(16) distance of 1.297 (8) Å. The short C(15)–C(16) distance of 1.407 (10) Å (1.396 (9) Å in **9**) shows that this bond also has a bond order larger than one. This points to a strong delocalization of electron density over the Fe–C(15)–C(16)N(3) part of the molecule.

Regarding the results reported by Daran et al. and those reported in this paper the question arises what causes the preference of MeC≡CNEt$_2$ for the coordination mode observed in **3b** and **9**, when coordinated to a dimetal fragment. The fact that in $Mo_2(OCH_2CMe_3)_6(\mu\text{-}\eta^1,\eta^2\text{-}NCNMe_2)$ a (dimethylamido)cyanide ligand is bonded to the dimolybdenum center in a similar fashion as the alkyne in **3b** and **9** suggests that the presence of a dialkylamido substituent plays a crucial role.[14] A theoretical study of this Mo complex indicates that the participation of the NMe$_2$ lone pair in the bonding of the NC–NMe$_2$ molecule is responsible for the ability of the molecule to coordinate to the $Mo_2(OR)_6$ fragment.[14] Although the results of the above-mentioned theoretical study cannot be directly applied to describe the bonding of the alkyne in **3b** and **9**, since the Mo—Mo—C—N part of the Mo_2 complex is planar whereas in **3b** the alkyne C=C bond is twisted with respect to the FeRu bond, we assume that the delocalization of the N lone pair over the N(3)—C(16), C(15)—C(16), and Fe—C(16) bonds causes the unusual coordination of the alkyne molecule.

A complex with an R$_2$N—C—CR ligand backbone similar to those in **3b** and **9**, i.e. $Fe_2(CO)_6(PPh_3)$(c-HexN-(H)CC(H)Ph) resulting from the nucleophilic attack of H$_2$N-c-Hex on the acetylide complex $Fe_2(CO)_6(PPh_2)$(C≡CPh), was reported several years ago.[15] Also in this complex there is a strong N=C double-bond character between the amine N atom and the acetylide C atom and a delocalization of negative charge over the reduced acetylide C—C bond.

Molecular Structure of $Fe_2(CO)_5$[*i*-PrNCHCHN-(*i*-Pr)C(O)C(Me)=CNEt$_2$] (8a). The crystal structure

Table V. Fractional Coordinates and Equivalent Isotropic Thermal Parameters of the Non-Hydrogen Atoms of 3b (Esd's in Parentheses)

atom	*x*	*y*	*z*	U_{eq}, Å^2
Ru(a)	0.17809 (4)	0.42595 (4)	0.17143 (5)	0.0416 (4)
Fe(a)	0.33743 (8)	0.24763 (9)	0.25420 (8)	0.0479 (8)
C(1a)	0.0773 (6)	0.4079 (7)	0.1843 (7)	0.072 (8)
C(2a)	0.1877 (6)	0.5131 (6)	0.2337 (6)	0.056 (6)
C(3a)	0.3757 (7)	0.5205 (7)	0.2687 (7)	0.077 (8)
C(4a)	0.3353 (6)	0.4097 (7)	0.1505 (6)	0.065 (7)
C(5a)	0.4245 (7)	0.3747 (8)	0.3026 (8)	0.086 (9)
C(6a)	0.1623 (6)	0.3578 (6)	0.0126 (6)	0.063 (7)
C(7a)	0.1617 (6)	0.4364 (7)	−0.0038 (6)	0.064 (7)
C(8a)	0.1636 (7)	0.2544 (6)	0.1008 (7)	0.066 (7)
C(9a)	0.0873 (9)	0.2186 4(8)	0.0431 (9)	0.109 (11)
C(10a)	0.2367 (8)	0.2142 (8)	0.0936 (8)	0.097 (10)
C(11a)	0.1574 (7)	0.5638 (7)	0.0359 (8)	0.075 (8)
C(12a)	0.2340 (8)	0.6028 (7)	0.0721 (9)	0.085 (9)
C(13a)	0.0848 (8)	0.5973 (7)	0.0478 (9)	0.087 (9)
C(14a)	0.2470 (8)	0.2853 (6)	0.3017 (6)	0.074 (7)
C(15a)	0.2486 (6)	0.3656 (5)	0.2779 (6)	0.051 (6)
C(16a)	0.2884 (5)	0.4195 (5)	0.3372 (6)	0.049 (6)
C(17a)	0.2275 (7)	0.4080 (7)	0.4474 (7)	0.072 (8)
C(18a)	0.1627 (9)	0.4633 (10)	0.4478 (10)	0.119 (14)
C(19a)	0.3453 (7)	0.4927 (6)	0.4609 (7)	0.068 (7)
C(20a)	0.4090 (8)	0.4553 (8)	0.5306 (8)	0.096 (10)
N(1a)	0.1680 (5)	0.3369 (4)	0.0868 (5)	0.049 (5)
N(2a)	0.1639 (5)	0.4808 (4)	0.0573 (5)	0.052 (5)
N(3a)	0.2871 4(5)	0.4376 (5)	0.4107 (4)	0.049 (5)
O(1a)	0.0178 (5)	0.4005 (7)	0.1981 (7)	0.127 (9)
O(2a)	0.1875 (5)	0.5681 (4)	0.2696 (5)	0.082 (5)
O(3a)	0.4007 (7)	0.5811 (6)	0.2821 (6)	0.123 (8)
O(4a)	0.3383 (4)	0.4001 (5)	0.0837 (4)	0.084 (6)
O(5a)	0.4821 (6)	0.3410 (7)	0.3339 (7)	0.134 (9)
Ru(b)	0.18080 (5)	0.21245 (5)	0.74943 (5)	0.0462 (4)
Fe(b)	0.27699 (8)	0.26907 (8)	0.66823 (8)	0.0474 (8)
C(1b)	0.1808 (7)	0.1474 (7)	0.8353 (7)	0.077 (8)
C(2b)	0.2414 (7)	0.2843 (7)	0.8250 (7)	0.071 (8)
C(3b)	0.2812 (7)	0.3659 (7)	0.6854 (7)	0.071 (8)
C(4b)	0.1847 (6)	0.2647 (6)	0.5872 (6)	0.065 (7)
C(5b)	0.3407 (7)	0.2611 (6)	0.6076 (7)	0.066 (7)
C(6b)	0.0278 (6)	0.1759 (6)	0.6280 (7)	0.065 (7)
C(7b)	0.0192 (6)	0.2519 (6)	0.6532 (7)	0.069 (7)
C(8b)	0.1071 (6)	0.0626 (7)	0.6479 (8)	0.072 (8)
C(9b)	0.1060 (9)	0.0513 (9)	0.5601 (9)	0.110 (11)
C(10b)	0.0436 (8)	0.0153 (7)	0.6695 (11)	0.105 (11)
C(11b)	0.0681 (8)	0.3586 (8)	0.7380 (9)	0.096 (10)
C(12b)	0.0140 (10)	0.3619 (9)	0.7866 (10)	0.120 (13)
C(13b)	0.0551 (11)	0.4156 (8)	0.6711 (12)	0.134 (14)
C(14b)	0.3060 (6)	0.0887 (7)	0.7047 (8)	0.074 (8)
C(15b)	0.2849 (5)	0.1679 (6)	0.7276 (6)	0.049 (6)
C(16b)	0.3448 (6)	0.2223 (6)	0.7625 (6)	0.056 (6)
C(17b)	0.4427 (9)	0.1578 (9)	0.8804 (10)	0.131 (12)
C(18b)	0.4051 (14)	0.1512 (15)	0.9393 (13)	0.204 (23)
C(19b)	0.4653 (8)	0.2890 (9)	0.8419 (11)	0.129 (12)
C(20b)	0.5327 (11)	0.2858 (11)	0.8177 (13)	0.159 (17)
N(1b)	0.0981 (5)	0.1445 (4)	0.6635 (5)	0.053 (5)
N(2b)	0.0791 (5)	0.2809 (5)	0.7091 (5)	0.063 (6)
N(3b)	0.4132 (5)	0.2233 (5)	0.8231 (6)	0.080 (6)
O(1b)	0.1862 (7)	0.1082 (6)	0.8904 (6)	0.123 (9)
O(2b)	0.2708 (6)	0.3284 (6)	0.8755 (6)	0.109 (7)
O(3b)	0.2843 (6)	0.4317 (5)	0.6972 (6)	0.115 (8)
O(4b)	0.1257 (5)	0.2630 (6)	0.5317 (5)	0.099 (6)
O(5b)	0.3822 (6)	0.2545 (6)	0.5674 (6)	0.113 (8)

(13) This bond length is comparable to those observed for other dinuclear complexes with a formally single Fe–Ru bond.[6]

(14) Chisholm, M. H.; Huffman, J. C.; Marchant, N. S. *Organometallics* **1987**, *6*, 1073.

(15) Carthy, A. J.; Mott, G. N.; Taylor, N. J.; Yule, J. E. *J. Am. Chem. Soc.* **1978**, *100*, 3051.

Table VI. Selected Bond Lengths (Å) of the Non-Hydrogen Atoms of Molecule A of 3b (Esd's in Parentheses)

Ru-Fe	2.693 (1)	C(7)-N(2)	1.294 (9)
Ru-C(15)	2.134 (7)	C(8)-N(1)	1.487 (9)
Ru-N(1)	2.105 (6)	C(11)-N(2)	1.51 (1)
Ru-N(2)	2.117 (6)	C(14)-C(15)	1.48 (1)
Fe-C(15)	2.037 (7)	C(15)-C(16)	1.407 (10)
Fe-C(16)	1.869 (7)	C(16)-N(3)	1.297 (8)
C(6)-C(7)	1.42 (1)	C(17)-N(3)	1.46 (1)
C(6)-N(1)	1.290 (9)	C(19)-N(3)	1.474 (10)

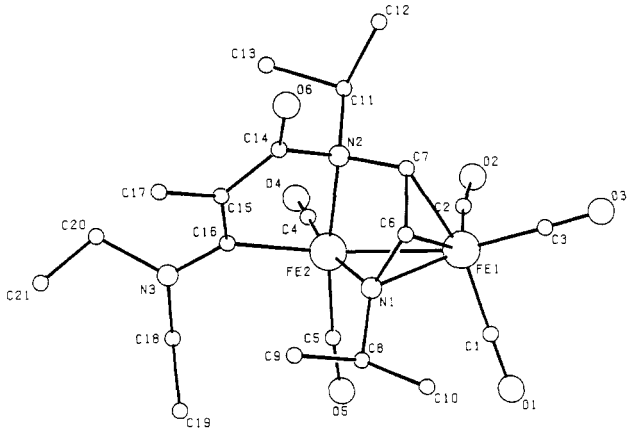

Figure 3. PLUTO drawing of molecule A of $Fe_2(CO)_5[i$-PrNCHCHN(i-Pr)C(O)C(Me)=CNEt$_2$] (**8a**). The H atoms are omitted for clairty.

of **8a** also shows two sets of two independent molecules, which are structurally identical apart from the conformations of the isopropyl and ethyl groups. Therefore in the following discussion only molecule A will be discussed.

The molecular strucutre of **8a** consists of an $Fe(CO)_3$ and an $Fe(CO)_2$ fragment that are linked by a formally single Fe–Fe bond [Fe(1)–Fe(2) = 2.576 (3) Å] and bridged by an organic ligand resulting from the coupling of the i-Pr-DAB ligand, a CO molecule, and a DEAP molecule. The N(1)–C(6)–C(7) part of the ligand is bonded as an azaalyl function to the $Fe(1)(CO)_3$ unit [Fe(1)–N(1) = 2.058 (8) Å; Fe(1)–C(6) = 2.03 (1) Å; Fe(1)–C(7) = 2.089 (9) Å; N(1)–C(6) = 1.40 (1) Å; C(6)–C(7) = 1.43 (1) Å] with N(1) bridging both metal centers [Fe(2)–N(1) = 1.958 (8) Å]. The second N atom of the DAB skeleton is σ-N bonded to Fe(2) [Fe(2)–N(2) = 2.033 (8) Å] and N–C coupled to a CO group. The same CO is C–C coupled to the CMe moiety of the DEAP, of which the CNEt$_2$ part has formed a σ-bond with Fe(2) [Fe(2)–C(16) = 1.96 (1) Å]. The bond lengths in the azaallyl part of the ligand are in agreement with those observed for other azaallyl complexes.[3i,16] The N(3)–C(16)–C(17)–C(15)–C(14)–O(6) part of the ligand is almost complete coplanar (root-mean-square deviation = 0.11 Å). This planarity facilitates delocalization of electron density, which is indeed observed. The bond lengths in the C(O)C(Me)=CNEt$_2$ part of the ligand indicate a strong delocalization over the N(3)—C(16)—C(15)—C(14) bonds, since both the N(3)—C(16) distance of 1.36 (1) Å and the C(15)—C(14) distance of 1.39 (1) Å are too short for single N—C and C—C bonds, respectively.[17] The origin of this delocalized electron density is no doubt the lone pair of the alkyne N atom, which is known to be able to participate easily in the bonding of aminoalkynes. The importance of the role of the N lone pair is corroborated by the fact that in similar M—N—C(O)C=C heterocycles formed

Table VII. Selected Bond Angles (deg) of the Non-Hydrogen Atoms of Molecule A of 3b (Esd's Parentheses)

Fe-Ru-C(1)	142.7 (3)	Ru-C(15)-Fe	80.4 (4)
Fe-Ru-C(2)	78.2 (3)	Ru-C(15)-C(14)	131.3 (5)
Fe-Ru-C(15)	48.2 (2)	Ru-C(15)-C(16)	107.1 (6)
Fe-Ru-N(1)	102.7 (2)	Fe-C(15)-C(14)	130.6 (6)
Fe-Ru-N(2)	106.4 (2)	Fe-C(15)-C(16)	62.6 (6)
C(1)-Ru-C(2)	89.8 (5)	C(14)-C(15)-C(16)	120.2 (8)
C(1)-Ru-C(15)	97.4 (5)	Fe-C(16)-C(15)	75.4 (6)
C(1)-Ru-N(1)	94.0 (4)	Fe-C(16)-N(3)	149.1 (5)
C(1)-Ru-N(2)	109.9 (4)	C(15)-C(16)-N(3)	135.0 (7)
C(2)-Ru-C(15)	90.4 (4)	Ru-N(1)-C(6)	114.8 (6)
C(2)-Ru-N(1)	171.9 (3)	Ru-N(1)-C(8)	128.7 (5)
C(2)-Ru-N(2)	96.1 (4)	C(6)-N(1)-C(8)	116.4 (7)
C(15)-Ru-N(1)	96.3 (4)	Ru-N(2)-C(7)	115.1 (6)
C(15)-Ru-N(2)	151.9 (3)	Ru-N(2)-C(11)	130.3 (5)
N(1)-Ru-N(2)	75.8 (3)	C(7)-N(2)-C(11)	114.7 (8)
Ru-Fe-C(15)	51.4 (2)	C(16)-N(3)-C(17)	123.3 (7)
Ru-Fe-C(16)	75.9 (3)	C(16)-N(3)-C(19)	120.5 (7)
C(15)-Fe-C(16)	42.0 (3)	C(17)-N(3)-C(19)	116.1 (8)

by the coupling of alkynes with no amino substituents, such an extensive delocalization as in **8a** is not observed.[18] An appropriate comparison of bond lengths, however, is hampered by the large variation of alkynes and N substrates used and by the fact that the reduced alkyne bond is in all cases η^2-C=C coordinated to a metal center.

The molecular structure of **8a** is reminiscent of that of two other complexes reported by us in the recent past, both derived from $M_2(CO)_6(i$-Pr-DAB) [M_2 = Fe_2, Ru_2]. The first is the product of the reaction of **1c** with H_2C=C=O, $Ru_2(CO)_5[i$-Pr-NCHCHN(i-Pr)C(O)CH$_2$C(O)CH$_2$] (**10**) which has, instead of the C(O)C(Me)=CNEt$_2$ fragment in **8a**, a head-to-tail coupled diketene fragment with a ketonic C atom bonded to the σ-N atom and a CH$_2$ group σ-bonded to Ru.[19] The second complex $Fe_2(CO)_5$-[Me$_2$C=NCHCHN-i-Pr][MeOC(O)C=CHC(O)OMe] (**11**) results from the thermal conversion of the initial product $Fe_2(CO)_5(i$-Pr-DAB)(μ_2,η^2-MeOC(O)C≡CC(O)OMe) of the reaction of **1a** with MeOC(O)C≡CC(O)OMe.[3h] This conversion comprises the migration of the methine H atom of one of the isopropyl groups to the alkyne. The latter two complexes **10** and **11** and **8a** have in common an azaallyl function coordinated to one metal center and an organic ligand σ-bonded to the other metal. The structural analogy is also shown by the similar ^{1}H and ^{13}C chemical shifts of the azaallyl moieties and the similar IR (ν_s (C=O)) patterns. Complexes **8a**, **10**, and **11** are schematically shown in Figure 4.

NMR Spectroscopy. Complexes **3b** and **3c** show a fluxional behavior in solution. For **3b** the ^{1}H NMR spectrum in the fast-exchange limit at 350 K shows a single resonance for the two imine protons and one septet for the i-Pr methine protons at 7.51 and 4.43 ppm, respectively. In the slow-exchange limit at 243 K these signals split in two singlets for the imine protons at 7.19 and 7.38 ppm and two septets for the i-Pr methine protons at 4.17 and 4.68 ppm. The coalescence temperatures of 268 K for the imine protons and 283 K for the methine protons at 100 MHz correspond with an activation energy for the averaging of the two halves of the DAB ligand of about 57.3 kJ·mol^{-1}. The much lower coalescence temperatures for **3c** or 197 and 208 K for the imine and methine protons, respectively, correspond with an activation energy for the

(16) Keijsper, J.; Mul, J.; van Koten, G.; Vrieze, K.; Ubbels, H. C.; Stam, C. H. *Organometallics* **1984**, *3*, 1732.
(17) *International Tables for X-Ray Crystallography*; Kynoch Press: Birmingham, England, 1974; Vol. III.

(18) (a) Dickson, R. S.; Nesbit, R. J.; Pateras, H.; Baimbridge, W.; Patrick, J. M.; White, A. H. *Organometallics* **1985**, *4*, 2128. (b) Han, S.-H.; Geoffroy, G. L.; Rheingold, A. L. *Organometallics* **1986**, *5*, 2561. (c) Nuel, D.; Dahan, F.; Mathieu, R. *Organometallics* **1986**, *5*, 1278.
(19) Polm, L. H.; van Koten, G.; Vrieze, K.; Stam, C. H.; van Tunen, W. C. J. *J. Chem. Soc., Chem. Commun.* **1983**, 1177.

Table VIII. Fractional Coordinates and Equivalent Isotropic Thermal Parameters of the Non-Hydrogen Atoms of 8a (Esd's in Parentheses)

atom	*x*	*y*	*z*	U_{eq}, Å^2
Fe(1a)	0.12438 (17)	−0.13673 (16)	0.31434 (17)	0.0480 (13)
Fe(2a)	0.22965 (15)	0.04010 (15)	0.33276 (16)	0.0395 (12)
N(1a)	0.0807 (8)	−0.0092 (8)	0.2991 (8)	0.038 (7)
N(2a)	0.2306 (8)	0.0297 (8)	0.4860 (8)	0.038 (7)
N(3a)	0.2833 (11)	0.2562 (9)	0.3397 (11)	0.067 (10)
C(1a)	0.0915 (13)	−0.1793 (13)	0.1745 (13)	0.075 (12)
C(2a)	0.2506 (11)	−0.1486 (11)	0.3491 (12)	0.055 (10)
C(3a)	0.0575 (14)	−0.2466 (11)	0.3384 (14)	0.072 (12)
C(4a)	0.3607 (11)	0.0582 (13)	0.3600 (13)	0.061 (11)
C(5a)	0.2150 (11)	0.0297 (11)	0.1940 (12)	0.051 (10)
C(6a)	0.0538 (11)	−0.0514 (10)	0.3820 (11)	0.047 (9)
C(7a)	0.1441 (9)	−0.0579 (10)	0.4643 (10)	0.039 (8)
C(8a)	−0.0031 (11)	0.0078 (12)	0.2080 (12)	0.057 (11)
C(9a)	−0.0229 (14)	0.1049 (13)	0.2477 (15)	0.083 (14)
C(10a)	−0.1032 (12)	−0.0755 (13)	0.1683 (13)	0.071 (12)
C(11a)	0.3285 (11)	0.0176 (11)	0.5667 (11)	0.046 (9)
C(12a)	0.3130 (12)	−0.0265 (12)	0.6670 (11)	0.057 (11)
C(13a)	0.4095 (12)	0.1193 (11)	0.6113 (12)	0.061 (11)
C(14a)	0.2010 (10)	0.1165 (10)	0.5276 (10)	0.041 (9)
C(15a)	0.2112 (12)	0.1930 (10)	0.4698 (12)	0.050 (10)
C(16a)	0.2441 (11)	0.1782 (10)	0.3806 (11)	0.048 (9)
C(17a)	0.1778 (17)	0.2828 (13)	0.5099 (16)	0.087 (16)
C(18a)	0.2958 (17)	0.2443 (13)	0.2309 (15)	0.090 (15)
C(19a)	0.1912 (17)	0.2403 (15)	0.1402 (16)	0.096 (16)
C(20a)	0.3483 (18)	0.3528 (14)	0.4125 (18)	0.106 (17)
C(21a)	0.3079 (26)	0.4308 (18)	0.3698 (21)	0.159 (26)
O(1a)	0.0655 (11)	−0.2091 (10)	0.0837 (10)	0.104 (10)
O(2a)	0.3293 (9)	−0.1679 (9)	0.3714 (9)	0.076 (8)
O(3a)	0.0167 (11)	−0.3213 (9)	0.3550 (12)	0.108 (11)
O(4a)	0.4464 (8)	0.0676 (9)	0.3709 (9)	0.080 (9)
O(5a)	0.2090 (9)	0.0151 (9)	0.1055 (8)	0.074 (8)
O(6a)	0.1693 (7)	0.1120 (7)	0.6059 (8)	0.055 (7)
Fe(1b)	0.33623 (18)	0.6576 (17)	0.11779 (18)	0.0518 (14)
Fe(2b)	0.28952 (16)	0.68729 (16)	−0.08005 (17)	0.0482 (13)
N(1b)	0.2954 (9)	0.5642 (8)	−0.0264 (10)	0.054 (8)
N(2b)	0.4450 (8)	0.7124 (8)	−0.0331 (9)	0.041 (7)
N(3b)	0.2300 (13)	0.6476 (15)	−0.3195 (11)	0.114 (14)
C(1b)	0.3405 (12)	0.7859 (11)	0.1256 (12)	0.055 (10)
C(2b)	0.4092 (13)	0.6494 (11)	0.2496 (14)	0.064 (12)
C(3b)	0.2212 (14)	0.6242 (16)	0.1531 (17)	0.091 (16)
C(4b)	0.1562 (11)	0.6654 (13)	−0.1000 (13)	0.064 (11)
C(5b)	0.2891 (13)	0.8085 (11)	−0.0969 (13)	0.059 (11)
C(6b)	0.3926 (11)	0.5651 (10)	0.0393 (11)	0.047 (10)
C(7b)	0.4584 (10)	0.6621 (10)	0.0601 (11)	0.042 (9)
C(8b)	0.2255 (14)	0.4601 (15)	−0.0540 (20)	0.122 (17)
C(9b)	0.2445 (16)	0.4098 (15)	−0.1549 (19)	0.115 (17)
C(10b)	0.1509 (32)	0.4369 (24)	−0.0404 (33)	0.292 (43)
C(11b)	0.5102 (11)	0.8175 (10)	−0.0065 (13)	0.054 (10)
C(12b)	0.6237 (13)	0.8314 (13)	0.0666 (16)	0.085 (13)
C(13b)	0.5114 (13)	0.8572 (12)	−0.1115 (14)	0.068 (12)
C(14b)	0.2976 (12)	0.6470 (12)	−0.2212 (12)	0.065 (11)
C(15b)	0.3887 (13)	0.6169 (13)	−0.2152 (13)	0.070 (12)
C(16b)	0.4681 (11)	0.6499 (10)	−0.1194 (12)	0.047 (10)
C(17b)	0.4100 (15)	0.5470 (15)	−0.2980 (15)	0.090 (15)
C(18b)	0.1269 (18)	0.6756 (18)	−0.3361 (17)	0.121 (19)
C(19b)	0.0457 (22)	0.5867 (20)	−0.3598 (20)	0.156 (23)
C(20b)	0.3025 (29)	0.6960 (20)	−0.4275 (19)	0.176 (27)
C(21b)	0.2324 (26)	0.6116 (23)	−0.4522 (37)	0.228 (39)
O(1b)	0.3520 (10)	0.8660 (8)	0.1475 (9)	0.081 (9)
O(2b)	0.4593 (11)	0.484 (10)	0.3358 (10)	0.100 (10)
O(3b)	0.1490 (13)	0.6027 (12)	0.1755 (15)	0.142 (15)
O(4b)	0.0735 (9)	0.6586 (9)	−0.1069 (11)	0.089 (9)
O(5b)	0.2837 (9)	0.8860 (9)	−0.1067 (10)	0.083 (9)
O(6b)	0.5538 (8)	0.6351 (7)	−0.0930 (8)	0.057 (7)

same process of 42.5 kJ·mol^{-1}. The ^{13}C NMR spectrum of **3b** shows that a second fluxional process involves the scrambling of the three CO ligands on Fe, which appear as a single resonance even at 243 K, the lowest temperature at which was measured. The ^{13}C spectrum also shows that the two CO ligands on Ru do not participate in the equilization of the two halves of the DAB ligand, since they are still observed as two single resonances when the DAB ligand is already in the fast-exchange limit at 323 K.

Table IX. Selected Bond Lengths (Å) of the Non-Hydrogen Atoms of Molecule A of 8a (Esd's in Parentheses)

Fe(1)–Fe(2)	2.576 (3)	N(2)–C(7)	1.48 (1)
Fe(1)–N(1)	2.058 (8)	N(2)–C(11)	1.53 (1)
Fe(1)–C(6)	2.03 (1)	N(2)–C(14)	1.50 (1)
Fe(1)–C(7)	2.089 (9)	N(3)–C(16)	1.36 (1)
Fe(2)–N(1)	1.958 (8)	C(6)–C(7)	1.43 (1)
Fe(2)–N(2)	2.033 (8)	C(14)–C(15)	1.39 (1)
Fe(2)–C(16)	1.96 (1)	C(14)–O(6)	1.24 (1)
N(1)–C(6)	1.40 (1)	C(15)–C(16)	1.40 (2)
N(1)–C(8)	1.49 (1)	C(15)–C(17)	1.56 (2)

Table X. Selected Bond Angles (deg) of the Non-Hydrogen Atoms of Molecule A of 8a (Esd's Parentheses)

Fe(2)–Fe(1)–N(1)	48.4 (3)	C(6)–N(1)–C(8)	118 (1)
Fe(2)–Fe(1)–C(6)	74.4 (4)	Fe(2)–N(2)–C(7)	100.1 (7)
Fe(2)–Fe(1)–C(7)	70.3 (4)	Fe(2)–N(2)–C(11)	117.7 (7)
N(1)–Fe(1)–C(6)	40.1 (4)	Fe(2)–N(2)–C(14)	107.7 (7)
N(1)–Fe(1)–C(7)	68.3 (5)	C(7)–N(2)–C(11)	111.0 (10)
C(6)–Fe(1)–C(7)	40.6 (5)	C(7)–N(2)–C(14)	109 (1)
Fe(1)–Fe(2)–N(1)	51.8 (3)	C(11)–N(2)–C(14)	111 (1)
Fe(1)–Fe(2)–N(2)	76.8 (3)	C(16)–N(3)–C(18)	122 (1)
Fe(1)–Fe(2)–C(4)	116.3 (5)	C(16)–N(3)–C(20)	122 (1)
Fe(1)–Fe(2)–C(5)	93.8 (5)	C(18)–N(3)–C(20)	114 (1)
Fe(1)–Fe(2)–C(16)	145.9 (3)	Fe(1)–C(6)–N(1)	70.8 (9)
N(1)–Fe(2)–N(2)	82.6 (5)	Fe(1)–C(6)–C(7)	71.7 (9)
N(1)–Fe(2)–C(4)	168.1 (5)	N(1)–C(6)–C(7)	110 (1)
N(1)–Fe(2)–C(5)	91.0 (6)	Fe(1)–C(7)–N(2)	107.3 (7)
N(1)–Fe(2)–C(16)	98.9 (6)	Fe(1)–C(7)–C(6)	67.7 (8)
N(2)–Fe(2)–C(4)	96.4 (7)	N(2)–C(7)–C(6)	112 (1)
N(2)–Fe(2)–C(5)	170.6 (4)	N(2)–C(14)–C(15)	114 (1)
N(2)–Fe(2)–C(16)	82.9 (5)	N(2)–C(14)–O(6)	118.1 (10)
C(4)–Fe(2)–C(5)	88.5 (8)	C(15)–C(14)–O(6)	128 (1)
C(4)–Fe(2)–C(16)	92.8 (8)	C(14)–C(15)–C(16)	117 (1)
C(5)–Fe(2)–C(16)	105.0 (7)	C(14)–C(15)–C(17)	115 (1)
Fe(1)–N(1)–Fe(2)	79.8 (5)	C(16)–C(15)–C(17)	128 (1)
Fe(1)–N(1)–C(6)	69.1 (8)	Fe(2)–C(16)–N(3)	127.9 (8)
Fe(1)–N(1)–C(8)	126.9 (7)	Fe(2)–C(16)–C(15)	112.4 (9)
Fe(2)–N(1)–C(6)	113.1 (8)	N(3)–C(16)–C(15)	120 (1)
Fe(2)–N(1)–C(8)	127.9 (7)		

Finally, it must be noticed that in the fast-exchange limit the two alkyne aminoethyl groups are still inequivalent on the NMR time scale in both the ^{1}H and ^{13}C NMR spectrum.

At 323 K still two Ru–CO resonances are observed with roughly the same chemical shift difference as the methine C atoms, which a 323 K are observed as one broad resonance. This enables us to conclude that the averaging of the two DAB halves does not involve the exchange of the two N atoms of the DAB ligand with the two CO ligands, since this process would, apart from both DAB halves, also make both CO's equivalent. This leaves only two other possible exchange mechanisms. One comprises the simple exchange of the two N sites on Ru. The second mechanism involves the fission of the Ru–C(15) bond after which the five-coordinate Ru center, which can be regarded as a distorted trigonal bipyramid, shows a number of Berry pseudorotations along the Fe–Ru, C(2)–Ru, and C(1)–Ru bonds, subsequently, resulting in the exchange of the σ-N sites and leaving the CO sites unaffected (see Figure 5). Since we are not able to compare the Ru–C(15) bond strength and the stability of the pseudorotation intermediates with the activation barrier of the simple rotation of the DAB ligand on Ru, it is not possible to assess with certainty which process is most likely.

The NMR data for **8a** are in agreement with its molecular structure in the solid state. The ketonic CO resonance is found at 212.9 ppm. This downfield shift may be the result of the earlier mentioned delocalization of the alkyne N lone pair over the conjugated organic fragment. The resulting relatively high electron density in a π-type orbital may cause a paramagnetic deshielding of the ke-

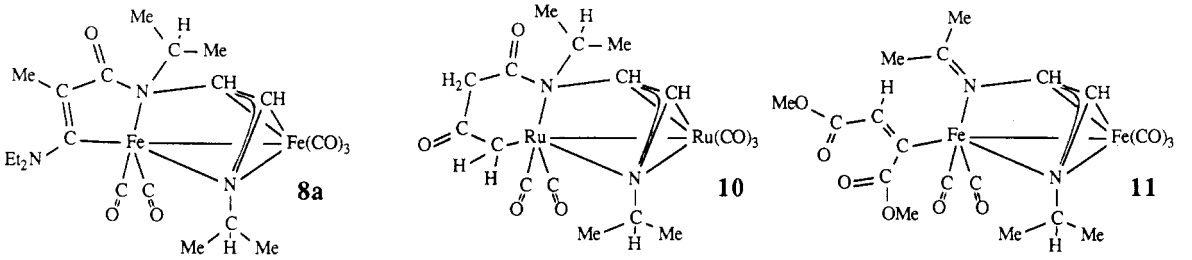

Figure 4. Compounds **8a**, **10**, and **11**.

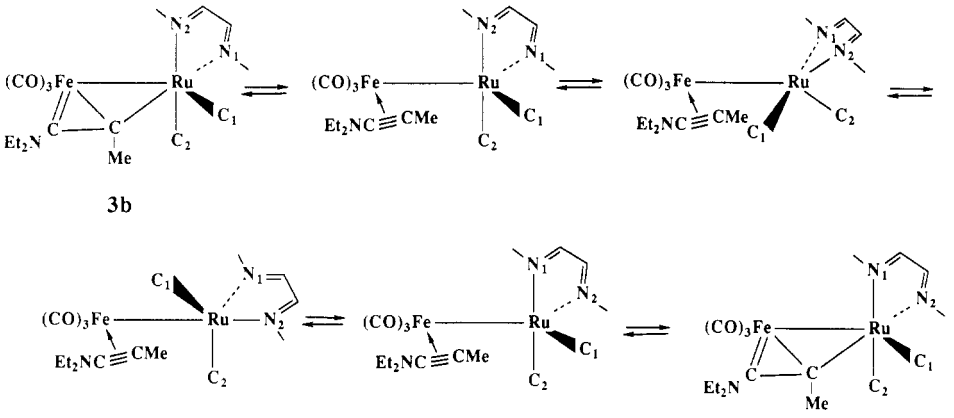

Figure 5. The pseudorotation exchange mechanism of the σ-N sites of **3b**.

tonic C nucleus and hence a downfield shift. The alkyne C atoms have chemical shifts of 102.3 and 180.7 ppm for the CMe and $CNEt_2$, respectively.

Complex Formation. The formation of the reported complexes in the reactions of $M_2(CO)_6$(*i*-Pr-DAB) [M_2 = Fe_2, FeRu, Ru_2] with DEAP appears to involve a common initial reaction step for all three complexes. This process comprises the substitution of the η^2-C=N coordinated imine moiety of the σ-N,μ_2-N′,η^2-C=N′ 6e donating DAB ligand in **1** by a η^2-C≡C monodentate bonded alkyne molecule to give intermediate **2** (see Scheme I). The coordination mode of the DAB ligand is changed to σ,σ-N,N′ chelating.

For $Ru_2(CO)_6$(*i*-Pr-DAB) (**1c**) the present reaction with DEAP is the first one involving the above-mentioned substitution changing the bonding mode of the DAB ligand from bridging to chelating in intermediate **2**.

The reactions of **1a** and **1b** with DEAP also proceed via the substitution of the η^2-C=N coordinated imine moiety by a DEAP molecule to give **2**. This is not surprising since even in reactions of **1a** and **1b** with activated alkynes like MeOC(O)C≡CC(O)OMe and MeOC(O)C≡CH, which react with **1c** to give the AIB complexes, no C—C coupling is observed. In these complexes a weaker π-backbonding, which is expected for Fe when compared to Ru, disfavors an electrophilic attack of the alkyne.

The supposed intermediate **2** cannot be isolated or observed spectroscopically and immediately loses a CO to give $M_2(CO)_5$(*i*-Pr-DAB)(MeC≡$CNEt_2$) (**3**), in which the alkyne takes in a 4e donating, bridging position. Products of this type can be isolated for FeRu (**3b**) and Ru_2 (**3c**), but not for M_2 = Fe_2. The complex $Fe_2(CO)_5$(*i*-Pr-DAB)(MeC≡$CNEt_2$) (**3a**) is apparently not formed at room temperature, but instead the formation of Fe_2-$(CO)_5$[*i*-Pr-NCHCH-N(*i*-Pr)C(O)C(Me)=$CNEt_2$] (**8a**) is observed, for which we propose the following mechanism: Intermediate **2** does not lose a CO to give **3** but instead gives a C—C coupling of the coordinated alkyne with one of the CO ligands resulting in a μ_2-Et_2NC=C(Me)C(O) fragment in **5a**. The η^2-C=C bonded olefinic part of this

Scheme II

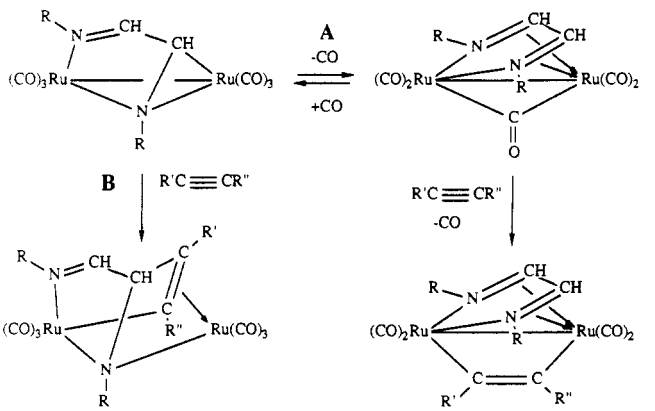

ligand is then substituted by the recoordination of one of the imine moieties of the DAB ligand to give **7a** after which the bridging N atoms is N–C coupled with the ketonic C atom, yielding **8a** (see Scheme I). This process is analogous to that proposed for the formation of the flyover complexes $Fe_2(CO)_5$[RN=CHCHN(R)C(O)CR′=CC(O)OMe] [R = *i*-Pr, c-Hex; R′ = H, C(O)OMe] in the reactions of Fe_2-$(CO)_6$(R-DAB) with MeOC(O)C≡CC(O)OMe and MeOC-(O)C≡CH.[3d,h] In the formation of **8a**, however, no flyover ligand results but instead the uncoupled CHCHN-*i*-Pr part of the DAB ligand becomes bonded as an azaallyl fragment.

At higher temperatures the formation of complex **3a** is apparently favored over the C–C coupling to give **5a**. Complex **3a** reacts further with a second alkyne molecule to give a head-to-tail coupling of the two alkynes resulting in the formation of the ferracyclopentadienyl complex Fe_2[MeC=C(NEt_2)C(Me)=$CNEt_2$]$(CO)_4$(*i*-Pr-DAB) (**6a**) (route C, see Scheme I).

We can, however, not exclude the possibility that the formation of **6a** proceeds via an intermediate $Fe_2(CO)_5$-(*i*-Pr-DAB)(μ_2,η^2-MeC≡$CNEt_2$) (**4a**) with a perpendicular bridging alkyne bonded in the same fashion as in Fe_2-

$(CO)_5$(*i*-Pr-DAB)(μ_2,η^2-MeOC(O)C≡CC(O)OMe) (route D, see Scheme II). It is known that this latter complex reacts with a second equivalent of alkyne to give various ferracyclopentadienyl compounds.[3f] Also the fact that **3b** and **3c** do not react with a second DEAP molecule, as was observed for **9**, suggests that **3a** is not involved in the formation of the ferracyclopentadienyl complex **6a**.

Conclusions

When we compare the reactivity toward dinuclear metal carbonyl α-diimine complexes of DEAP, with electron-donating substituents, with that of alkynes with electron-withdrawing substituents, it becomes clear that the electronic properties of the alkyne used have a major influence on the chosen reaction path. The different behavior of DEAP with respect to that of alkynes with electron-withdrawing substituents becomes especially clear in the reaction with $Ru_2(CO)_6$(*i*-Pr-DAB) which leads to the first example of the substitution of the η^2-C=N bonded imine fragment by an alkyne. Because of the δ^- polarization of the alkyne C atoms it does not lead to an electrophilic attack of the alkyne on the coordinated imine C atom resulting in a C–C coupling as observed for activated alkynes. The crystal structures of **3b** and **8a** have clearly shown the importance of the participation of the alkyne N lone pair in the bonding of the alkyne. For **3b** this leads to a unique coordination mode which as yet has only been observed for this type of alkyne.

Acknowledgment. The Institute for Mass Spectrometry of the University of Amsterdam is thanked for measuring the FI mass spectra. We are indebted to Dr. C. H. Stam of the Laboratory for Crystallography of the University of Amsterdam for revising the crystallographic data. Dr. H.-W. Frühauf is thanked for critically revising the manuscript.

Registry No. **1a**, 74552-74-2; **1b**, 90219-33-3; **1c**, 74552-69-5; **3b**, 119656-29-0; **3c**, 119656-30-3; **6a**, 119679-59-3; **8a**, 119656-31-4; DEAP, 4231-35-0.

Supplementary Material Available: Tables of the anisotropic thermal parameters of the non-hydrogen atoms, full listings of the bond lengths, full listings of bond angles of the non-hydrogen atoms, and stereoscopic ORTEP representations of molecule A for **3b** and **8a** and a table of the calculated fractional coordinates of the hydrogen atoms for **3b** (9 pages); listings of observed and calculated structure factors for **3b** and **8a** (53 pages). Ordering information is given on any current masthead page.